

CoRL-MPPI: Enhancing MPPI With Learnable Behaviours For Efficient And Provably-Safe Multi-Robot Collision Avoidance

Stepan Dergachev, Artem Pshenitsyn, Aleksandr Panov, Alexey Skrynnik, Konstantin Yakovlev

Abstract—Decentralized collision avoidance is a core challenge for scalable multi-robot systems. One of the promising approaches to tackle this problem is Model Predictive Path Integral (MPPI) – a framework that naturally handles arbitrary motion models and provides strong theoretical guarantees. Still, in practice MPPI-based controller may provide suboptimal trajectories as its performance relies heavily on uninformed random sampling. In this work, we introduce CoRL-MPPI, a novel fusion of Cooperative Reinforcement Learning and MPPI to address this limitation. We train an action policy (approximated as deep neural network) in simulation that learns local cooperative collision avoidance behaviors. This learned policy is then embedded into the MPPI framework to guide its sampling distribution, biasing it towards more intelligent and cooperative actions. Notably, CoRL-MPPI preserves all the theoretical guarantees of regular MPPI. We evaluate our approach in dense, dynamic simulation environments against state-of-the-art baselines, such as ORCA, BVC, RL-RVO-NAV and classical MPPI. Our results demonstrate that CoRL-MPPI significantly improves navigation efficiency (measured by success rate and makespan) and safety, enabling agile and robust multi-robot navigation.

I. INTRODUCTION

The deployment of multi-robot systems promises significant boost in efficiency in such domains as warehouse logistics, search-and-rescue, disaster management etc. A fundamental problem in any multi-robot system is decentralized collision avoidance: each robot must navigate to its goal while ensuring safety by proactively avoiding conflicts with others. This problem is inherently challenging due to the non-linear and dynamic nature of robot interactions, the curse of dimensionality as the number of agents increases, and the necessity for real-time computation under uncertainty.

The known approaches to this problem are mostly reactive. Typical examples include Velocity Obstacles and Optimal Reciprocal Collision Avoidance (ORCA) [1], which compute collision-free velocities based on the current states of neighboring robots. Another line of research considers methods based on Buffered Voronoi Cells (BVC) [2], which construct safe operating regions for each agent at every step. While highly computationally efficient, reactive methods are inherently myopic. They operate on a one-step time horizon, which can lead to oscillatory behavior, deadlocks, and a general lack of cooperation.

Conversely, methods based on receding-horizon optimal control, most notably the Model Predictive Control (MPC) framework, explicitly optimize a trajectory over multiple steps while accounting for predicted future states. The Model Predictive Path Integral (MPPI) [3], a sampling-based variant of MPC, has gained a significant attention for its ability to

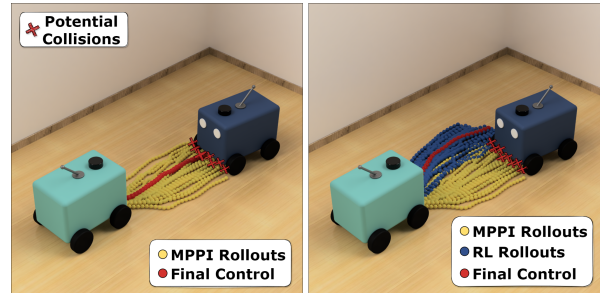


Fig. 1: Left – the standard MPPI controller, where random rollouts (yellow) lead to potential collisions (red crosses) and suboptimal control (red trajectory); right – the proposed fusion of RL and MPPI, where learned policy rollouts (blue) bias the sampling distribution toward more cooperative and collision-free behaviors.

handle non-linear dynamics and complex cost functions without the need for gradient computation. MPPI allows flexible formulation of both motion models and cost functions and is widely used in mobile robotics.

However, the performance of MPPI-based methods is critically dependent on the quality of its sampled trajectories. In its standard formulation, control sequences are drawn from a Gaussian distribution centered around a prior (often the previous solution). Such sampling may be very inefficient in complex multi-agent settings, where the vast majority of sampled trajectories may lead to uncooperative behavior. Consequently, even when the number of samples is high the resultant trajectories may be overly egoistic leading to an overall degradation of the multi-robot system’s performance. Generally, one may claim that *MPPI in multi-robot navigation lacks an understanding of multi-agent cooperation*.

Meanwhile, recent advances in Reinforcement Learning have demonstrated remarkable success in learning complex, cooperative behaviors directly from simulation. RL-based agents may learn implicit cooperation strategies, learning to anticipate the actions of other agents and negotiate passage efficiently. Yet, purely learned policies are often sensitive to distribution shifts and poor performance in new environments not seen during training. Moreover, they typically lack the guarantees provided by the model-based controllers.

To this end, we propose a novel hybrid approach to multi-robot collision avoidance, that leverages the complementary strengths of both paradigms – CoRL-MPPI. We believe we are the first to develop such an approach in decentralized, partially observable multi-agent setting. In CoRL-MPPI, first,

a learnable policy is obtained that encapsulates the high-level strategic knowledge of cooperative avoidance, and then CoRL-MPPI additionally uses the distribution of controls from this policy for sampling. Thus the search is biased towards intelligent and cooperative trajectories – see Fig 1. Overall, in CoRL-MPPI the learnable policy provides the strategic intuition of the cooperative behavior while MPPI provides the robust long-horizon planning with the full model dynamics and ensures formal safety guarantees.

To summarize, the core contributions of this paper are:

- We introduce CoRL-MPPI, a novel hybrid architecture that integrates a learned RL policy into the MPPI control framework to guide its sampling distribution for decentralized multi-robot navigation.
- We provide theoretical justification that CoRL-MPPI preserves safety guarantees; moreover, when execution noise is present, control safety is maintained with a specified probability.
- A comprehensive empirical evaluation in simulation demonstrating that CoRL-MPPI outperforms classical approaches (e.g. ORCA, BVC), learnable approaches (e.g., RL-RVO-NAV [4] and the standalone RL policy used for guidance) and an MPPI-based multi-agent collision-avoidance baseline [5] in terms of success rate and navigation efficiency (makespan).
- We further validate CoRL-MPPI in a physics-based Gazebo simulation with multiple robots integrated into the ROS2 navigation stack, demonstrating collision-free navigation and real-time control performance in a realistic robotics pipeline.

II. RELATED WORK

a) Model Predictive Path Integral: The Model Predictive Path Integral (MPPI) algorithm was originally proposed as a sampling-based optimal control method [3] and later extended to Information-Theoretic MPC to handle general non-linear dynamics [6]. Since then, numerous extensions have been proposed to improve smoothness, robustness, and sampling efficiency, including SMPPI [7], CC-MPPI [8], Tube-MPPI [9], Robust-MPPI [10] and CBF-MPPI [11], [12].

Although most MPPI-based methods have been developed for single-agent systems, several studies have explored their adaptation to multi-agent scenarios. These works typically address dynamic collision avoidance, either assuming explicit inter-agent communication [13], [14], [15] or relying on motion prediction without formal safety guarantees [16]. A notable exception is the decentralized MPPI-ORCA framework [17], [5], which provides theoretical safety guarantees through the incorporation of ORCA-based constraints. However, this method still relies on the basic MPPI sampling scheme, which can lead to inefficiencies in complex interaction scenarios.

Recent research has also investigated the integration of reinforcement learning into the MPPI framework. For instance, TD-MPC [18] and TD-MPC2 [19] learn a latent

dynamics model and a value function to perform short-horizon rollouts, achieving high sample efficiency but lacking formal safety guarantees. RL-driven MPPI [20], which is the closest approach to ours, combines an offline RL policy with MPPI by using the learned policy for trajectory generation and the RL value function as a terminal cost. While this reduces reliance on random sampling, it is limited to fully observable single-agent settings, lacks safety guarantees, and depends heavily on the generalization capability of the learned RL policy.

b) Multi-Agent Collision Avoidance: Multi-agent navigation with collision avoidance is an important problem in robotics. The main goal is to move several agents safely in a shared continuous space without collisions.

Velocity-based approaches define a set of admissible velocities that guarantee collision-free motion and then select the optimal velocity within this feasible region. One of the most established representatives of this class is the Optimal Reciprocal Collision Avoidance (ORCA) algorithm [1], which provides an efficient solution for reciprocal collision avoidance. Despite its popularity, ORCA does not take into account kinematic limitations of agents. To partially overcome these drawbacks, Snape et al. [21], [22] proposed modifying ORCA for differential-drive robots by expanding the effective agent radius, thereby indirectly modeling non-holonomic constraints. The Non-Holonomic ORCA (NH-ORCA) algorithm [23], [24] extends this concept by explicitly considering non-holonomic motion through the use of precomputed lookup tables that encode feasible velocities. Other variants, such as PRVO [25], CALU [26], and COCALU [27], incorporate uncertainty in localization and sensing into the velocity-obstacle framework.

Another family of methods, based on BVC [2], defines safe navigation zones by constructing buffered Voronoi regions around each agent. The PBVC algorithm [28] extends this principle to a decentralized formulation that accounts for perception uncertainty, but it neglects kinematic constraints. A more recent modification, B-UAVC [29], integrates positional uncertainty and can be adapted to different motion models. However, the general B-UAVC formulation relies on Model Predictive Control (MPC), requiring the development of a dedicated MPC controller consistent with the agent’s dynamic model.

In addition, several learning-based methods [30], [31], [32], [33], [4] have been proposed to address the multi-agent collision avoidance problem. Some of them operate directly on raw sensory inputs (e.g., LiDAR) [31], [32], thereby eliminating the need for explicit state estimation. For instance, Han et al. [4] combine decentralized reinforcement learning with reciprocal velocity obstacles to reduce collisions. Nevertheless, such approaches lack formal safety guarantees and often rely purely on reactive behaviors learned from training data, which may fail to generalize to unseen scenarios.

III. PROBLEM STATEMENT

Consider a set of homogeneous robots (agents) $\mathcal{A} = \{1, 2, \dots, N\}$, operating in a two-dimensional workspace

$\mathcal{W} \subset \mathbb{R}^2$. Each robot is modeled as a disk of radius r . Time is discretized, and at each step, every robot selects a control (action) $\mathbf{u}_t \in \mathbb{R}^m$ to update its state $\mathbf{x}_t \in \mathbb{R}^n$. However, the executed control is subject to stochastic perturbations that model actuation uncertainty:

$$\mathbf{v}_t \sim \mathcal{N}(\mathbf{u}_t, \Sigma), \quad \Sigma = \text{diag}(\sigma_1^2, \dots, \sigma_m^2) \quad (1)$$

where $\mathbf{v}_t \in \mathbb{R}^m$ represents the actual, randomly perturbed control signal.

The robot dynamics is described in a general form as:

$$\mathbf{x}_{t+1} = F(\mathbf{x}_t) + G(\mathbf{x}_t)\mathbf{v}_t, \quad (2)$$

where $F: \mathbb{R}^n \rightarrow \mathbb{R}^n$ and $G: \mathbb{R}^n \rightarrow \mathbb{R}^{n \times m}$ are given functions (capturing robot's kinematic and dynamic constraints); and the control input is bounded:

$$\mathbf{v}_{\min}[k] \leq \mathbf{v}_t[k] \leq \mathbf{v}_{\max}[k] \quad (3)$$

where $[k]$ denotes the k -th element of a vector.

At each time step, robot i has perfect knowledge of its own state \mathbf{x}_t^i and can perceive the relative positions \mathbf{p}_t^j and velocities \mathbf{v}_t^j of the nearby robots (within a certain range).

The control \mathbf{u}_t^i robot i is said to be *probabilistically safe* (or simply *safe*) with respect to robot j if, after executing the perturbed control $\mathbf{v}_t \sim \mathcal{N}(\mathbf{u}_t, \Sigma)$ and transitioning to the next state \mathbf{x}_{t+1}^i , the probability that the inter-robot distance falls below $2r$ does not exceed a predefined threshold δ .

The problem now is to compute, at each time step, a control input \mathbf{u}_t^i for every robot $i \in \mathcal{A}$ such that (i) it satisfies the control constraints given by (3); (ii) it ensures progress toward the assigned goal τ_i ; (iii) it remains probabilistically safe with respect to all observed neighboring robots.

IV. BACKGROUND

Our method is based on Model Predictive Path Integral (MPPI) control and Reinforcement Learning (RL). We begin by providing a brief overview of MPPI.

A. Model-Predictive Path Integral

The MPPI algorithm addresses a discrete-time stochastic optimal control problem formulated as:

$$u^* = \arg \min_{u \in \mathcal{U}^H} \mathbb{E} \left[\phi(\mathbf{x}_H) + \sum_{t=0}^{H-1} \left(q(\mathbf{x}_t) + \frac{\gamma}{2} \mathbf{u}_t^T \Sigma^{-1} \mathbf{u}_t \right) \right], \quad (4)$$

where \mathcal{U} denotes the set of admissible controls, $u = (\mathbf{u}_0, \dots, \mathbf{u}_{H-1})$ represents the control sequence, $x = (\mathbf{x}_0, \dots, \mathbf{x}_H)$ is the corresponding trajectory over a prediction horizon of length H , $\phi(\cdot)$ denotes the terminal cost, $q(\cdot)$ is the running cost, and $\gamma \in \mathbb{R}^+$ is the control cost weight parameter.

Let \mathbf{x}_0 denote the current system state and $u^{init} = (\mathbf{u}_0^{init}, \dots, \mathbf{u}_{H-1}^{init})$ an initial control sequence. The MPPI framework generates K stochastic perturbations $\xi^k = (\boldsymbol{\varepsilon}_0^k, \dots, \boldsymbol{\varepsilon}_{H-1}^k)$, with each noise term sampled as $\boldsymbol{\varepsilon}_t^k \sim \mathcal{N}(0, \Sigma^*)$. Here, the sampling covariance Σ^* is a scaled version of the nominal control noise covariance Σ (matrix Σ^* must remain diagonal).

Using these samples, a set of K candidate control sequences $\{u^k\}_{k=1}^K$ is obtained as: $u^k = (\mathbf{u}_0^k, \dots, \mathbf{u}_{H-1}^k)$, $\mathbf{u}_t^k = \mathbf{u}_t^{init} + \boldsymbol{\varepsilon}_t^k$

Each sampled control sequence induces a trajectory x^k through the system dynamics, and is assigned a scalar trajectory cost $S(x^k, u^k)$ (the exact information-theoretic form of S and the role of control penalties are standard and can be found in the original MPPI derivations [6]).

The updated control sequence is then obtained as an importance-weighted average of the sampled perturbations, the importance weights for which are computed based on $S(x, u)$. After executing the first control \mathbf{u}_0^* , the initial control sequence is updated $u^{init} = (\mathbf{u}_1^*, \dots, \mathbf{u}_{H-1}^*, \mathbf{u}^{init})$.

Pure MPPI does not guarantee collision avoidance because sampling may generate unsafe controls. To address this, we adopt the distribution-shaping approach proposed in [17], [5].

During the MPPI sampling process, the parameters of the control distribution, denoted as $\hat{\mathbf{u}}_t^{init}$ and $\hat{\Sigma}^*$, are adjusted to remain close to the nominal ones $\mathbf{u}_t^{init}, \Sigma^*$, while simultaneously increasing the likelihood of satisfying predefined safety constraints. In this work, safety constraints are represented using the ORCA-based linear inequalities in the velocity space [1]. The determination of the adjusted parameters is formulated as the convex optimization problem [5].

Solving this optimization problem yields updated parameters $\hat{\mathbf{u}}_t^{init}$ and $\hat{\Sigma}^*$ of the sampling distribution such that, with some desired probability, the sampled control inputs satisfy all safety constraints.

B. Reinforcement Learning

The problem introduced in Section III, i.e. decentralized multi-agent navigation with collision avoidance, can be formulated as a decentralized partially observable Markov decision process (Dec-POMDP) [34], [35]. Formally, Dec-POMDP is defined as a tuple $(\mathbb{X}, \{\mathbb{U}^i\}_{i=1}^N, \mathbb{T}, \mathfrak{R}, \{\Omega^i\}_{i=1}^N, \gamma)$, where $\mathbb{X} \ni \mathbf{x}_t$ is the global state space, $\mathbb{U}^i \ni \mathbf{u}_t^i$ is the action space of agent i , $\mathbb{U} = \times^i \{\mathbb{U}^i\}_{i=1}^N \ni \mathbf{u}_t^\times$ is the joint action space, $\mathbb{T}(\mathbf{x}_{t+1} | \mathbf{x}_t, \mathbf{u}_t^\times)$ is the transition model, $\mathfrak{R}(\mathbf{x}_t, \mathbf{u}_t^\times, \mathbf{x}_{t+1})$ is the reward function, $\Omega^i: \mathbb{X} \rightarrow \mathbb{O}^i \ni \mathbf{o}_t^i$ is the observation function of agent i , $\gamma \in [0, 1)$ is the discount factor.

State space \mathbb{X} contains the states of all agents and environment properties that matter for navigation and collisions. For example, agent positions \mathbf{p}_t^i , velocities \mathbf{v}_t^i , safe radii r^i , obstacles in the workspace, etc. Dynamics \mathbb{T} describes how the system transitions from one state to another based on the actions (controls) picked by the agents. In the considered case \mathbb{T} is defined by Eq. 2.

To reflect the requirements of the collision-avoidance problem, the reward function should penalize agents for collisions and encourage them for successfully reaching their destinations. Each agent has partial and local information as an observation. Ω^i returns the observation \mathbf{o}_t^i for agent i . It can include its own state \mathbf{x}_t^i , and relative positions \mathbf{p}_t^j and velocities \mathbf{v}_t^j of nearby agents $j \neq i$.

At each timestep t , each agent i selects an action (control) $\mathbf{u}_t^i \in \mathbb{U}^i$ using its policy $\pi^i(\mathbf{o}_t^i)$. The joint action \mathbf{u}_t^\times drives

the next state via \mathbb{T} . Then each agent gets a new observation, and a team receives a scalar reward.

The goal is to learn decentralized policies $\{\pi^i\}_{i=1}^N$ that maximize the expected discounted return under the Dec-POMDP dynamics and partial observations. We define the joint policy as $\pi^\times = \times^i \pi^i$ meaning that each agent selects actions from its own policy based only on its local observation, and the joint action is sampled from the product distribution. A clear statement is

$$\times^i \pi^i(\mathbf{o}^i) = \arg \max_{\mathbf{u}_t^\times \sim \times^i \pi^i} \sum_t [\gamma^t \mathfrak{R}(\mathbf{x}_t, \mathbf{u}_t^\times, \mathbf{x}_{t+1})] \quad (5)$$

There are many ways to solve the optimization problem in Eq. 5. One strong family is policy gradient methods that directly improve a parameterized policy by ascending the expected return. Proximal Policy Optimization (PPO) [36] is a strong actor-critic approach that uses a clipped surrogate loss to make updates stable and effective.

Many Multi-agent RL (MARL) methods build on policy gradients, and several use PPO to handle multi-agent problems, including centralized critic PPO, parameter sharing PPO, etc. A simple yet effective choice is Independent PPO (IPPO) [37], where each agent learns its own policy and value from local observations, and treats other agents as part of the environment. Let agent i use policy $\pi_{\theta^i}(\mathbf{o}_t^i)$ and value $V_{\phi^i}(\mathbf{o}_t^i)$. The clipped surrogate loss, value loss, and total loss are:

$$\begin{cases} \mathbf{L}_\pi^i(\theta^i) = \mathbb{E} \left[\min(\rho_i^i A_t^i, \text{clip}(\rho_i^i, 1 - \varepsilon, 1 + \varepsilon) A_t^i) \right], \\ \mathbf{L}_V^i(\phi^i) = \mathbb{E} \left[\left(V_{\phi^i}(\mathbf{o}_t^i) - V_{\text{target}}(\mathbf{o}_t^i) \right)^2 \right], \\ \mathbf{L}_{\text{total}} = \sum_{i=1}^N (\mathbf{L}_\pi^i(\theta^i) + \lambda_1 \mathbf{L}_V^i(\phi^i) + \lambda_2 \mathbf{H}(\pi_{\theta^i})) \end{cases} \quad (6)$$

where $\rho_i^i = \frac{\pi_{\theta^i}}{\pi_{\theta^i}^{\text{old}}}$ denotes a probability ratio, ε is a clip range hyperparameter, A_t^i - a GAE- λ estimator of the advantage function [38], $V_{\text{target}}(\mathbf{o}_t^i)$ - bootstrapped return target, $\mathbf{H}(\pi_{\theta^i})$ - an entropy bonus for agent i , λ_1, λ_2 are value loss weight and entropy bonus weight, respectively.

V. CoRL-MPPI: COOPERATIVE RL-GUIDED MPPI FOR MULTI-AGENT COLLISION AVOIDANCE

The suggested method, CoRL-MPPI, relies on dual-branch prediction structure in which both the MPPI-based sequence and the RL-guided sequence evolve over the full prediction horizon and undergo multi-step safety refinement. Specifically, we, first, learn a decentralized navigation and collision avoidance policy via reinforcement learning and, second, use the distribution of actions provided by the trained policy in the MPPI framework. This ensures that even the RL-derived proposal distribution remains probabilistically safe throughout the planning horizon, preserving the theoretical guarantees of MPPI while benefiting from the cooperative behavior captured by the learned policy. Noteworthy, CoRL-MPPI, is easy to comprehend, implement, and re-use.

A. Pre-trained RL-based Policy

Each agent's observation is represented as a vector encoding information about its goal and nearby agents. Specifically, each observation includes the relative distance and angular offset to the goal, as well as to the k nearest agents within a local sensing range. All components of the observation vector are normalized to ensure numerical stability and invariance to environment scale.

Each agent's action consists of continuous control variables corresponding to its motion commands. These actions are bounded within predefined intervals appropriate for the agent's dynamic model used during training.

At every simulation step, the reward for agent i is defined as a weighted sum of components encouraging goal reaching and smooth navigation while penalizing collisions and violations of social distance to nearby agents:

$$\mathfrak{R}^i = \mathfrak{R}_{\text{on.g}}^i - \mathfrak{R}_{\text{collision}}^i - \mathfrak{R}_{\text{social.dist}}^i + \mathfrak{R}_{\text{g.dist}}^i;$$

The formulation is compatible with different dynamic models and control parameter choices, since it only needs the state and neighbor information available in the simulator. A single policy shared among all agents is trained using IPPO as described in the background section.

B. Multi-Step Safety-Constrained and RL-Guided Planning Step

Consider the planning step for agent i . First, we predict the future positions of every neighboring agent for the planning horizon $t = 0, \dots, H$. We do this by employing the constant-velocity prediction model:

$$\mathbf{p}_{t+1}^j = \mathbf{p}_t^j + \mathbf{v}_t^j, \quad \forall j \in \mathcal{A}_i \quad \forall t = 0, \dots, H \quad (7)$$

Next, two predictive trajectories, x^{mppi} and x^π , are constructed. The first trajectory, x^{mppi} , follows the previously optimized control sequence u^{init} (see Section IV-A). A corresponding sequence of covariance matrices Σ^{mppi} is also maintained:

$$u^{\text{mppi}} = u^{\text{init}}, \quad \Sigma^{\text{mppi}} = \{\Sigma_t^* = \Sigma_{t=0}^*\}_{t=0}^{H-1} \quad (8)$$

The second trajectory, x^π , along with the control and variance sequences u^π and Σ^π , is generated using the pre-trained RL policy π . For this purpose, the predicted positions \mathbf{p}_{t-1}^j of neighboring agents, the previous trajectory element \mathbf{x}_{t-1}^π , and the goal position τ are combined into an observation vector \mathbf{o}_t . The policy then outputs the parameters of the control distribution:

$$(u^\pi, \Sigma^\pi) = \{(u_t^\pi, \Sigma_t^\pi) = \pi(\mathbf{x}_t^\pi, \mathbf{o}_t)\}_{t=0}^{H-1}. \quad (9)$$

For each time step within the safety horizon H_{safe} , the mean controls $\hat{\mathbf{u}}_t^{\text{mppi}}$, $\hat{\mathbf{u}}_t^\pi$ and corresponding covariances $\hat{\Sigma}_t^{\text{mppi}}$, $\hat{\Sigma}_t^\pi$ for both sampling branches are refined by solving the optimization problem [5], which enforces probabilistic safety constraints to ensure collision-free behavior.

An illustration of this adjustment process is shown in Figure 2. Initially, when sampling from both distributions $\mathcal{N}(\mathbf{u}_t^\pi, \Sigma_t^\pi)$ and $\mathcal{N}(\mathbf{u}_t^{\text{mppi}}, \Sigma_t^{\text{mppi}})$, there is a high probability

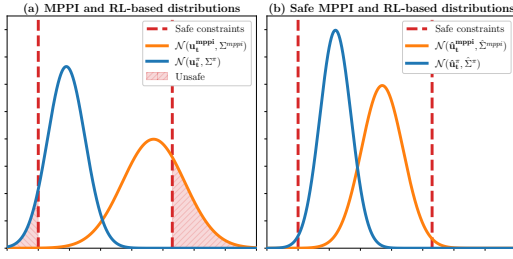


Fig. 2: Control distributions before and after applying safety constraints. (a) Original MPPI and RL-based distributions, with unsafe probability mass shown in red. (b) Distributions after the safety-constrained update, where the unsafe mass is removed to satisfy the required confidence level. Dashed lines indicate the safety bounds.

of generating unsafe controls. After applying the optimization procedure, the updated distributions $\mathcal{N}(\hat{\mathbf{u}}_t^\pi, \hat{\Sigma}_t^\pi)$ and $\mathcal{N}(\hat{\mathbf{u}}_t^{\text{mppi}}, \hat{\Sigma}_t^{\text{mppi}})$ reduce the likelihood of unsafe samples to the specified safety level δ .

Both trajectories are propagated forward over the prediction horizon H using the robot’s dynamic model (2):

$$\mathbf{x}_t^\pi = F(\mathbf{x}_{t-1}^\pi) + G(\mathbf{x}_{t-1}^\pi)\hat{\mathbf{u}}_{t-1}^\pi \quad (10)$$

$$\mathbf{x}_t^{\text{mppi}} = F(\mathbf{x}_{t-1}^{\text{mppi}}) + G(\mathbf{x}_{t-1}^{\text{mppi}})\hat{\mathbf{u}}_{t-1}^{\text{mppi}} \quad (11)$$

Subsequently, two sets of control rollouts, $\{u^k\}_{k=1}^{K^\pi}$ and $\{u^k\}_{k=K^\pi}^K$, are sampled: one around the RL-guided control sequence $\hat{\mathbf{u}}_t^\pi$ with variances $\hat{\Sigma}_t^\pi$, and another around the MPPI-based sequence $\hat{\mathbf{u}}_t^{\text{mppi}}$ with variances $\hat{\Sigma}_t^{\text{mppi}}$. Each sampled control sequence u^k induces a trajectory x^k , which is evaluated using the MPPI cost function $S(x^k, u^k)$. The resulting costs are transformed into trajectory weights $\omega(x^k, u^k)$, and the final control sequence u^* is obtained as a weighted average of all sampled controls. After executing the first control action \mathbf{u}_0^* , the optimized sequence is shifted forward and reused as the initialization for the next planning iteration.

VI. EXPERIMENTAL EVALUATION

A. Benchmarking in Numerical Simulation

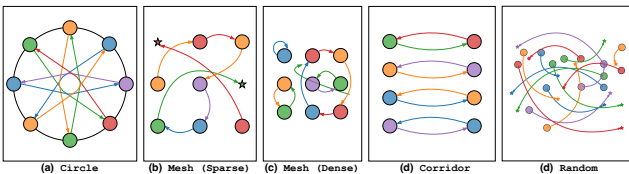


Fig. 3: Illustrative visualization of the experimental scenarios. Scales and proportions are adjusted for clarity

a) **Experimental Setup:** In the experiments, a differential-drive robot model was employed. We use this model as it is widely adopted in mobile robotics and enables direct comparison with a large body of prior multi-robot navigation methods that assume the same kinematics.

The agent’s state, denoted as \mathbf{x} , was defined as $\mathbf{x} = (p_x, p_y, \theta)^T$, where p_x and p_y represent the robot’s position (the center of the corresponding disk) in a two-dimensional workspace, and θ denotes the robot’s heading angle. The control input was defined as $\mathbf{u} = (v, w)^T$, where v and w correspond to the linear and angular velocities, respectively.

At each time step, the selected control input was perturbed by zero-mean Gaussian noise $\varepsilon \sim \mathcal{N}(0, \Sigma)$. The resulting control commands were constrained according to the following bounds, consistent with (3). The robot’s motion was governed by the discrete-time kinematic model:

$$\mathbf{x}_{t+1} = \mathbf{x}_t + \begin{pmatrix} \cos \theta_t & 0 \\ \sin \theta_t & 0 \\ 0 & 1 \end{pmatrix} (\mathbf{u}_t + \varepsilon). \quad (12)$$

All robots in the experiments shared identical physical and control parameters: the robot size (radius of the disk) was set to $r = 0.3\text{m}$; linear velocity limits were $v_{\min} = -1.0\text{m/s}$ and $v_{\max} = 1.0\text{m/s}$; angular velocity limits were $w_{\min} = -2.0\text{rad/s}$ and $w_{\max} = 2.0\text{rad/s}$; and the control noise covariance was $\Sigma = \text{diag}(0.1\text{m/s}, 0.2\text{rad/s})^2$. The observation radius was assumed to be unbounded. The simulation time step was fixed at 0.1s

b) **Experimental Environments:** Five types of scenarios were used for training and/or evaluation: Circle, Mesh (Sparse and Dense), Corridor, and Random. An illustrative depiction of these scenarios is presented in Figure 3.

In Circle scenario, N agents are placed uniformly on a circle and must reach diametrically opposite goals, which induces dense interactions near the center and often leads to symmetric deadlocks. This scenario was used for both training and evaluation. Training used diameters of 14m and 20m with 32 agents. For evaluation, the diameter was fixed at 14m and N varied from 5 to 50 in steps of 5 (10 repeats per setting).

In Mesh, agents start at cell centers of a square grid with zero initial heading and are assigned goals by a random permutation of grid cells. The Sparse mesh, used for training, employed a 6×6 grid with a cell size of 2m and 32 agents, leaving some cells unoccupied. Dense scenario, used for evaluation, includes a smaller cell size (1.5m) with all cells occupied and grids from 2×2 to 5×5 (10 instances, 10 runs each).

In Corridor, agents are arranged into two parallel rows facing each other, separated by 14m, with 1m spacing within each row. Robots in rows must swap positions. This scenario was not used for training and serves only for evaluation, with N ranging from 4 to 40 in steps of 4 (10 runs each).

Finally, in Random scenario N agents and their goals are sampled uniformly in a $40\text{m} \times 40\text{m}$ area. We tested $N \in \{10, 20, 30, 40, 50\}$, generating 10 instances per setting and executing each instance 10 times.

Lets note, that the choice of the sparse scenario for training was intentional: it provides an intermediate level of interaction complexity while encouraging meaningful cooperative behaviors. We then evaluate the learned policy on both denser

(Mesh (Dense)) and sparser settings (Random) to assess generalization across different interaction densities.

c) RL Policy Training Details: To obtain the pre-trained policy used in our method, we trained decentralized agents in the CAMAR environment [39] using a differential-drive dynamic model. We employed the parameter shared IPPO [37] algorithm implemented in the Sample Factory framework [40]. Agents share network parameters but use their own observations and rewards.

The observation space was modified compared to the default CAMAR setup, as described in V-A. Additionally, distances were normalized by dividing by the sensing range radius, and all angular quantities were scaled to the interval $[-1, 1]$.

Similarly, we used a slightly adapted reward function, as described in V-A, where the terms are defined as:

$$\begin{cases} \mathcal{R}_{\text{on-g}}^i &= 1.75, \text{ if } \|\mathbf{x}_{t+1}^i - \boldsymbol{\tau}_i\| \leq r_\tau; \\ \mathcal{R}_{\text{collision}}^i &= 4.6, \text{ if } \exists j \in N : \|\mathbf{x}_{t+1}^i - \mathbf{x}_{t+1}^j\| < r^i + r^j; \\ \mathcal{R}_{\text{social.dist}}^i &= 4.0 \cdot \frac{PS^i - d_{\min}^i}{PS^i}, \text{ if } d_{\min}^i \leq PS^i; \\ \mathcal{R}_{\text{g.dist}}^i &= 3.7 \cdot (\|\mathbf{x}_t^i - \boldsymbol{\tau}_i\| - \|\mathbf{x}_{t+1}^i - \boldsymbol{\tau}_i\|). \end{cases}$$

We define the size of the personal space $PS^i = 3.0 \cdot r^i$ and the distance to the nearest agent $d_{\min}^i = \min_{j \neq i} \|\mathbf{x}_{t+1}^i - \mathbf{x}_{t+1}^j\|$.

We trained a single RL policy on tasks with 32 agents for 60M environment steps ($\approx 1.9B$ individual agent steps). Each episode consisted of 1,500 simulation steps. The training utilized 128 parallel vectorized environments, running on a single NVIDIA H100 GPU. Owing to Sample Factory’s high-throughput asynchronous architecture and the efficiency of the CAMAR simulator, the entire training process completed in under 2 hours.

d) Implementation Details: The CoRL-MPPI was implemented in C++. The ONNX Runtime framework [41] was employed for executing the inference of the pre-trained policy.

The cost function $S(x, u)$ comprised several components: (i) a running cost penalizing the deviation of trajectory positions from the target, (ii) a running cost inversely proportional to the distance to the nearest predicted position of a neighboring agent, (iii) a running cost inversely proportional to the *mean* distance to neighboring agents, (iv) a collision penalty based on predicted neighboring trajectories, (v) a running cost encouraging passing other agents on the left-hand side, (vi) a penalty on abrupt changes of the motion direction at the first control step, and (vii) a terminal cost penalizing the deviation of the final trajectory position from the target.

In the experiments, a time horizon of 30 steps (corresponding to 3 seconds) was used, with 1000 sampled rollouts per iteration. Among these, 30% of the trajectories were sampled from the RL-guided distribution. Safety constraints were enforced for the first 3 steps of the prediction horizon.

e) Baselines: We compare our method with ORCA-DD [21], B-UAVC [29], RL-RVO-NAV [4] and a multi-agent collision avoidance algorithm based on the MPPI framework MPPI-ORCA (the version from [5]). Addi-

tionally, we include RL-POLICY as a baseline, i.e., the standalone RL strategy used within our method.

ORCA-DD is derived from the well-known ORCA [1] algorithm, but it uses an inflated agent radius to account for kinematic constraints.

The B-UAVC method builds on the BVC approach and incorporates several enhancements, particularly the consideration of kinematic constraints for differential-drive robots.

RL-RVO-NAV is a decentralized reinforcement-learning method for multi-robot navigation that uses RVO-inspired features to produce collision-avoiding control commands from local observations. We include it as a representative learning-based baseline.

To ensure a fair comparison, MPPI-ORCA was configured identically to our CoRL-MPPI algorithm in terms of cost design and MPPI parameters. This algorithm incorporated control execution noise, while the neighbors’ positions were assumed to be known exactly.

ORCA-DD and B-UAVC methods have been modified in such a way that a small random value $\epsilon_x, \epsilon_y \sim \mathcal{N}(0, 0.3)$ is added to the goal direction vector. This was necessary to reduce the chance of getting into deadlocks in symmetric cases. In addition, for all non-learning methods involved in the experiment, the radius of the agent used in the computations was increased by $\epsilon_r = 0.01 m$ relative to the real radius to minimize the chance of collision by creating additional safety buffer.

f) Experimental Results: The primary performance metrics evaluated in the experiments were the **success rate** and the **makespan**. The **success rate** represents the proportion of launches in which all agents successfully reached their respective goals without collisions, within a tolerance of 0.3, m, and before reaching the predefined limit of 1000 simulation steps. After reaching their goals, agents were allowed to depart from them. The **makespan** denotes the total time required for all agents to reach their respective goals. In addition, the presence of collisions during execution was analyzed to assess both the safety of the compared approaches.

The resulting **success rates** are summarized in Table I, along with the proportion of runs terminated due to collisions. Among the tested environments, the Random scenario proved to be the least challenging for all algorithms. In contrast, the Circle and Mesh (Dense) scenarios, which involve complex deadlock resolution and dense agent interactions, were considerably more difficult.

CoRL-MPPI achieved flawless performance across all scenarios, completing all tasks without any collisions. Its predecessor, MPPI-ORCA, demonstrated comparable performance, with 100% success and 0% collisions across all evaluated scenarios. In contrast, ORCA-DD and B-UAVC showed substantially lower success rates, particularly in more complex scenarios: for example, in the CIRCLE scenario, ORCA-DD reached only 66% success with 15% collisions, while B-UAVC achieved 40% success with 57% collisions. The learnable baselines performed even worse; RL-RVO-NAV had 25% success with 70% collisions in the Mesh

Algorithm	Random		Corridor		Circle		Mesh (Dense)	
	SR \uparrow	% Col. \downarrow	SR \uparrow	% Col. \downarrow	SR \uparrow	% Col. \downarrow	SR \uparrow	% Col. \downarrow
ORCA-DD	99.8%	0%	73%	0%	66%	15%	46.5%	0%
B-UAVC	96.8%	0.8%	100%	0%	40%	57%	54.5%	27.75%
RL-RVO-NAV	74%	26%	85%	3%	19%	81%	25%	70%
RL-POLICY	37.6%	62%	85%	15%	74%	26%	2.5%	97.5%
MPPI-ORCA	100%	0%	100%	0%	100%	0%	100%	0%
CoRL-MPPI	100%	0%	100%	0%	100%	0%	100%	0%

TABLE I: Success rate and percentage of runs terminated due to collisions for the evaluated algorithms. The arrows indicate preferred directions of improvement.

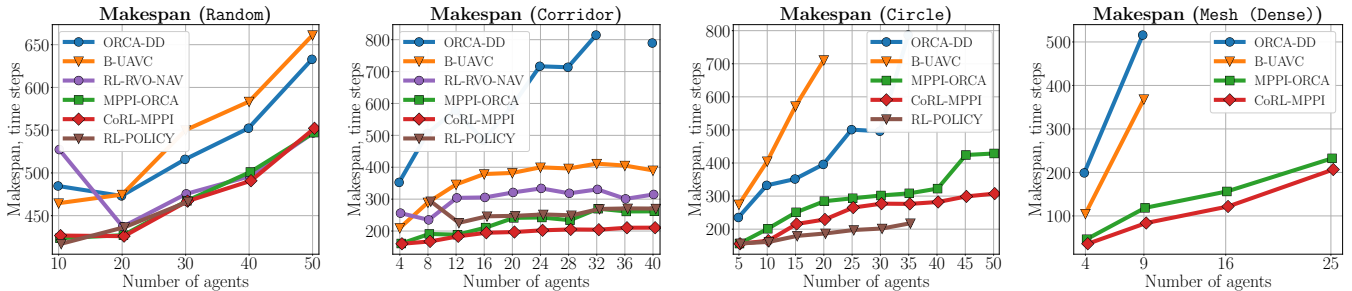


Fig. 4: The average makespan of the evaluated algorithms. The lower is better.

(Dense) scenario, and RL-POLICY achieved only 2.5% success with 97.5% collisions in the same scenario. Methods with provable collision guarantees, such as CoRL-MPPI and MPPI-ORCA, clearly ensure safe navigation; however, it is necessary to further study their performance.

Figure 4 reports the average **makespan** as a function of the number of agents. A data point is shown only if it meets the following threshold criteria. For single-task scenarios, we require at least 50% successful runs. For multi-task scenarios, we keep only tasks where each algorithm achieves at least 50% successful runs; additionally, an algorithm is omitted at a given agent count if it succeeds on fewer than 50% of the remaining tasks. For clarity, we also hide algorithms that produce too few valid points in a scenario, as the resulting sparse curves are not informative.

Overall, the makespan results are consistent with the success-rate trends observed earlier. CoRL-MPPI and MPPI-ORCA perform comparably on Random tasks, but on the Mesh (Dense), Corridor and Circle scenarios, CoRL-MPPI achieves better performance. Notably, for the largest number of agents, CoRL-MPPI outperforms MPPI-ORCA by nearly $1.25\times$ in the Corridor and $1.4\times$ in the Circle scenario, demonstrating improved efficiency while maintaining perfect collision avoidance.

Other baselines are also exceeded in most settings, particularly in the structured, interaction-heavy scenarios (Corridor, Circle, and Mesh (Dense)), where coordination and deadlock resolution are critical.

Two points are worth noting. First, in Random, MPPI-ORCA and the RL-based baselines achieve makespan comparable to the proposed approach; this is expected in a low-density environment where interactions are relatively

weak and cooperative behavior is less critical. Second, RL-POLICY is competitive on Circle for smaller teams, likely because this scenario was included during training. However, as the number of agents increases, RL-based methods begin to incur collisions, highlighting the limitations of purely learnable approaches in dense multi-agent settings.

The figures clearly illustrate that MPPI-based approaches outperform the competing methods. It is also worth noting that large-scale sparse configurations similar to the Random scenario were not included in the RL policy’s training process. Nevertheless, the proposed approach maintained comparable performance to the classical method, demonstrating strong generalization capability. In contrast, in densely populated scenarios requiring coordinated decision-making, the proposed method outperforms all competitors.

B. Physics-Based Simulation

In addition, we validated the proposed approach in a physics-based robotic simulation (Gazebo) with ten differential-drive TurtleBot3 robots. Our controller was integrated into the ROS2 Navigation Stack (Nav2) [42] as a custom local controller module. Global guidance was provided by a simple straight-line reference toward each goal. To supply inter-robot state information, we subscribed to ground-truth neighbor poses published on dedicated ROS topics at 8 ms intervals.

Experiments were performed in the Circle scenario. Figure 5 illustrates (i) this setup in Gazebo and (ii) the local observations of a single robot and the trajectory rollouts generated during CoRL-MPPI optimization. Two clearly separated rollout branches are visible: one produced by the standard MPPI sampling process, and a second set biased by the RL-guided proposal. (iii) Our method consistently

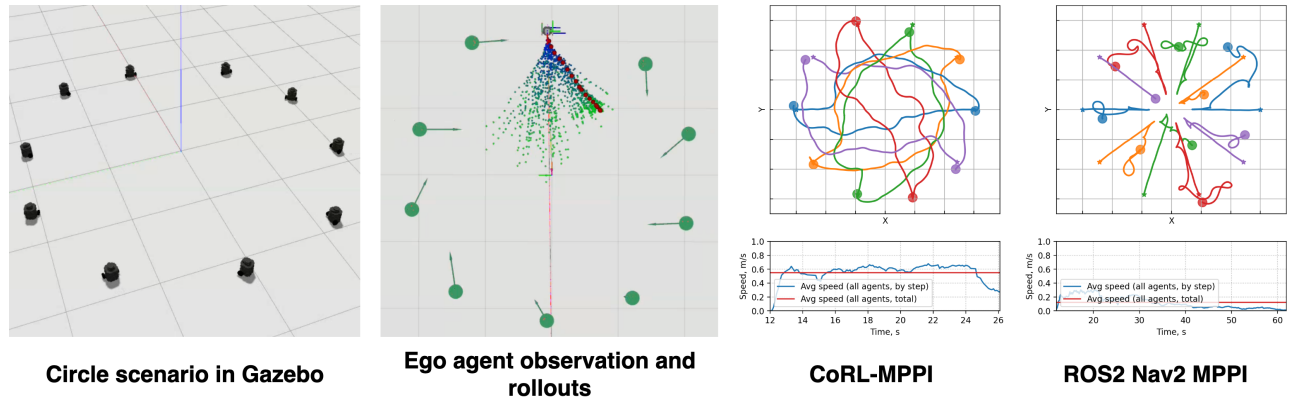


Fig. 5: Simulation in Gazebo. (i) 10 Turtlebots in Circle scenario, (ii) Single agent observation and CoRL-MPPI rollouts, (iii)-(iv) trajectories for the CoRL-MPPI and the built-in Nav2 MPPI Controller, respectively.

brought all robots to their assigned targets without collisions while preserving real-time operation with control update rate above 10 Hz. (iv) By comparison, the built-in Nav2 MPPI controller struggled to resolve multi-robot interactions.

VII. CONCLUSIONS

In this work we have introduced CoRL-MPPI – a novel hybrid framework that enhances the Model Predictive Path Integral controller with learnable, cooperative behaviors for decentralized multi-robot collision avoidance. Our approach successfully addresses a key limitation of vanilla MPPI – its reliance on uninformed random sampling – by leveraging a pre-trained reinforcement learning policy to intelligently bias the sampling distribution. Extensive simulation experiments in dense and dynamic scenarios confirm that the suggested method significantly outperforms state-of-the-art baselines, including ORCA, BVC, and a decentralized multi-agent MPPI implementation. Promising directions include deploying suggested method on physical robot swarms to bridge the sim-to-real gap and investigating the online adaptation of the policy to further improve generalization across diverse and evolving environments.

REFERENCES

- [1] J. Van Den Berg, S. J. Guy, M. Lin, and D. Manocha, “Reciprocal n-body collision avoidance,” in *Robotics Research: The 14th International Symposium ISRR*. Springer, 2011, pp. 3–19.
- [2] D. Zhou, Z. Wang, S. Bandyopadhyay, and M. Schwager, “Fast, on-line collision avoidance for dynamic vehicles using buffered voronoi cells,” *IEEE Robotics and Automation Letters*, vol. 2, no. 2, pp. 1047–1054, 2017.
- [3] G. Williams, P. Drews, B. Goldfain, J. M. Rehg, and E. A. Theodorou, “Aggressive driving with model predictive path integral control,” in *2016 IEEE International Conference on Robotics and Automation (ICRA)*, 2016, pp. 1433–1440.
- [4] R. Han, S. Chen, S. Wang, Z. Zhang, R. Gao, Q. Hao, and J. Pan, “Reinforcement learned distributed multi-robot navigation with reciprocal velocity obstacle shaped rewards,” *IEEE Robotics and Automation Letters*, vol. 7, no. 3, pp. 5896–5903, 2022.
- [5] S. Dergachev and K. Yakovlev, “Decentralized uncertainty-aware multi-agent collision avoidance with model predictive path integral,” 2025. [Online]. Available: <https://arxiv.org/abs/2507.20293>
- [6] G. Williams, N. Wagener, B. Goldfain, P. Drews, J. M. Rehg, B. Boots, and E. A. Theodorou, “Information theoretic mpc for model-based reinforcement learning,” in *2017 IEEE International Conference on Robotics and Automation (ICRA)*, 2017, pp. 1714–1721.
- [7] T. Kim, G. Park, K. Kwak, J. Bae, and W. Lee, “Smooth model predictive path integral control without smoothing,” *IEEE Robotics and Automation Letters*, vol. 7, no. 4, pp. 10 406–10 413, 2022.
- [8] J. Yin, Z. Zhang, E. Theodorou, and P. Tsiotras, “Trajectory distribution control for model predictive path integral control using covariance steering,” in *2022 International Conference on Robotics and Automation (ICRA)*, 2022, pp. 1478–1484.
- [9] I. M. Balci, E. Bakolas, B. Vlahov, and E. A. Theodorou, “Constrained covariance steering based tube-mpci,” in *2022 American Control Conference (ACC)*, 2022, pp. 4197–4202.
- [10] M. S. Gandhi, B. Vlahov, J. Gibson, G. Williams, and E. A. Theodorou, “Robust model predictive path integral control: Analysis and performance guarantees,” *IEEE Robotics and Automation Letters*, vol. 6, no. 2, pp. 1423–1430, 2021.
- [11] C. Tao, H. Kim, H. Yoon, N. Hovakimyan, and P. Voulgaris, “Control barrier function augmentation in sampling-based control algorithm for sample efficiency,” in *2022 American Control Conference (ACC)*, 2022, pp. 3488–3493.
- [12] C. Tao, H.-J. Yoon, H. Kim, N. Hovakimyan, and P. Voulgaris, “Path integral methods with stochastic control barrier functions,” in *2022 IEEE 61st Conference on Decision and Control (CDC)*, 2022, pp. 1654–1659.
- [13] Z. Wang, A. D. Saravanos, H. Almarak, O. So, and E. A. Theodorou, “Sampling-based optimization for multi-agent model predictive control,” *arXiv preprint arXiv:2211.11878*, 2022.
- [14] L. Song, P. Zhao, N. Wan, and N. Hovakimyan, “Safety embedded stochastic optimal control of networked multi-agent systems via barrier states,” in *2023 American Control Conference (ACC)*, 2023, pp. 2554–2559.
- [15] I. S. Mohamed, M. Ali, and L. Liu, “Chance-constrained sampling-based mpc for collision avoidance in uncertain dynamic environments,” *IEEE Robotics and Automation Letters*, vol. 10, no. 7, pp. 7492–7499, 2025.
- [16] L. Streichenberg, E. Trevisan, J. J. Chung, R. Siegwart, and J. Alonso-Mora, “Multi-agent path integral control for interaction-aware motion planning in urban canals,” in *2023 IEEE International Conference on Robotics and Automation (ICRA)*, 2023, pp. 1379–1385.
- [17] S. Dergachev and K. Yakovlev, “Model predictive path integral for decentralized multi-agent collision avoidance,” *PeerJ Computer Science*, vol. 10, p. e2220, 2024.
- [18] N. Hansen, X. Wang, and H. Su, “Temporal difference learning for model predictive control,” *arXiv preprint arXiv:2203.04955*, 2022.
- [19] N. Hansen, H. Su, and X. Wang, “Td-mpc2: Scalable, robust world models for continuous control,” *arXiv preprint arXiv:2310.16828*, 2023.
- [20] Y. Qu, H. Chu, S. Gao, J. Guan, H. Yan, L. Xiao, S. E. Li, and J. Duan, “RL-driven MPPI: Accelerating online control laws calculation with offline policy,” *IEEE Transactions on Intelligent Vehicles*, vol. 9, no. 2, pp. 3605–3616, 2024.
- [21] J. Snape, J. Van Den Berg, S. J. Guy, and D. Manocha, “Smooth and collision-free navigation for multiple robots under differential-drive constraints,” in *2010 IEEE/RSJ international conference on intelligent robots and systems*, 2010, pp. 4584–4589.

- [22] J. Snape, S. J. Guy, J. Van Den Berg, and D. Manocha, "Smooth coordination and navigation for multiple differential-drive robots," in *Experimental Robotics: The 12th International Symposium on Experimental Robotics*, 2014, pp. 601–613.
- [23] J. Alonso-Mora, A. Breitenmoser, M. Ruffi, P. Beardsley, and R. Siegwart, "Optimal reciprocal collision avoidance for multiple non-holonomic robots," in *Distributed autonomous robotic systems: The 10th international symposium*, 2013, pp. 203–216.
- [24] J. Alonso-Mora, P. Beardsley, and R. Siegwart, "Cooperative collision avoidance for nonholonomic robots," *IEEE Transactions on Robotics*, vol. 34, no. 2, pp. 404–420, 2018.
- [25] B. Gopalakrishnan, A. K. Singh, M. Kaushik, K. M. Krishna, and D. Manocha, "Prvo: Probabilistic reciprocal velocity obstacle for multi robot navigation under uncertainty," in *2017 IEEE/RSJ International Conference on Intelligent Robots and Systems (IROS)*, 2017, pp. 1089–1096.
- [26] D. Hennes, D. Claes, W. Meeussen, and K. Tuyls, "Multi-robot collision avoidance with localization uncertainty," in *Proceedings of the 11th International Conference on Autonomous Agents and Multiagent Systems-Volume 1*, 2012, pp. 147–154.
- [27] D. Claes, D. Hennes, K. Tuyls, and W. Meeussen, "Collision avoidance under bounded localization uncertainty," in *2012 IEEE/RSJ International Conference on Intelligent Robots and Systems*, 2012, pp. 1192–1198.
- [28] M. Wang and M. Schwager, "Distributed collision avoidance of multiple robots with probabilistic buffered voronoi cells," in *2019 international symposium on multi-robot and multi-agent systems (MRS)*, 2019, pp. 169–175.
- [29] H. Zhu, B. Brito, and J. Alonso-Mora, "Decentralized probabilistic multi-robot collision avoidance using buffered uncertainty-aware voronoi cells," *Autonomous Robots*, vol. 46, no. 2, pp. 401–420, 2022.
- [30] Y. F. Chen, M. Liu, M. Everett, and J. P. How, "Decentralized non-communicating multiagent collision avoidance with deep reinforcement learning," in *Proceedings of the 2017 IEEE International Conference on Robotics and Automation (ICRA) 2017*, 2017, pp. 285–292.
- [31] P. Long, T. Fan, X. Liao, W. Liu, H. Zhang, and J. Pan, "Towards optimally decentralized multi-robot collision avoidance via deep reinforcement learning," in *2018 IEEE international conference on robotics and automation (ICRA)*, 2018, pp. 6252–6259.
- [32] T. Fan, P. Long, W. Liu, and J. Pan, "Distributed multi-robot collision avoidance via deep reinforcement learning for navigation in complex scenarios," *The International Journal of Robotics Research*, vol. 39, no. 7, pp. 856–892, 2020.
- [33] S. Asayesh, M. Chen, M. Mehrandezh, and K. Gupta, "Least-restrictive multi-agent collision avoidance via deep meta reinforcement learning and optimal control," in *International Conference on Robot Intelligence Technology and Applications*, 2022, pp. 213–225.
- [34] D. S. Bernstein, R. Givan, N. Immerman, and S. Zilberstein, "The complexity of decentralized control of markov decision processes," *Mathematics of operations research*, vol. 27, no. 4, pp. 819–840, 2002.
- [35] L. P. Kaelbling, M. L. Littman, and A. R. Cassandra, "Planning and acting in partially observable stochastic domains," *Artificial intelligence*, vol. 101, no. 1-2, pp. 99–134, 1998.
- [36] J. Schulman, F. Wolski, P. Dhariwal, A. Radford, and O. Klimov, "Proximal policy optimization algorithms," *arXiv preprint arXiv:1707.06347*, 2017.
- [37] C. S. De Witt, T. Gupta, D. Makoviichuk, V. Makoviychuk, P. H. Torr, M. Sun, and S. Whiteson, "Is independent learning all you need in the starcraft multi-agent challenge?" *arXiv preprint arXiv:2011.09533*, 2020.
- [38] J. Schulman, P. Moritz, S. Levine, M. Jordan, and P. Abbeel, "High-dimensional continuous control using generalized advantage estimation," *arXiv preprint arXiv:1506.02438*, 2015.
- [39] A. Pshenitsyn, A. Panov, and A. Skrynnik, "Camar: Continuous actions multi-agent routing," *arXiv preprint arXiv:2508.12845*, 2025.
- [40] A. Petrenko, Z. Huang, T. Kumar, G. Sukhatme, and V. Koltun, "Sample factory: Egocentric 3d control from pixels at 100000 fps with asynchronous reinforcement learning," in *International Conference on Machine Learning*. PMLR, 2020, pp. 7652–7662.
- [41] O. R. developers, "Onnx runtime," <https://onnxruntime.ai/>, 2021, version: x.y.z.
- [42] S. Macenski, F. Martin, R. White, and J. Ginés Clavero, "The marathon 2: A navigation system," in *2020 IEEE/RSJ International Conference on Intelligent Robots and Systems (IROS)*, 2020.